Wellbore Integrity in at the Krechba Carbon Storage Site, In Salah, Algeria: 2. Reactive Transport Modeling of Geochemical Interactions Near the Cement – Formation Interface

Walt W. McNab[1] and Susan A. Carroll[1]

Lawrence Livermore National Laboratory, Livermore, California, USA.

Abstract

A reactive transport modeling approach was used to assess key geochemical reactions between wellbore cement, formation mineralogy, and injected supercritical CO_2 at the Krechba natural gas field at In Salah, Algeria. Characterization of these reactions is important for understanding changes in porosity and permeability and the propagation or sealing of fractures in the formation or wellbore cement. Experiments involving the reaction of CO_2 with reservoir mineral assemblages and wellbore cement under *in situ* conditions, combined with geochemical modeling, were used to identify candidate reactive mineral phases and reaction rates specifically applicable to CO_2 injection at In Salah. These findings informed a reactive transport model which considered advective transport of CO_2 along the wellbore-formation interface and diffusive transport of CO_2 and brine constituents into juxtaposed wellbore cement. Model results indicate shallow carbonation of the cement along the interface, leading to appreciable changes in cement porosity. Diffusive transport of cations such as Ca, Fe, and Al between the cement and formation materials results in mineralogical changes in the formation material immediately adjacent to the cement, including localized dissolution of calcite and precipitation of siderite, magnesite, gibbsite, smectite, and amorphous silica. In contrast to the cement, the modeled porosity changes in the formation material appear to be minor. Taken together, these results suggest (1) significant retardation of the rate of advance of CO_2 along the interface, and (2) relatively minor impacts to permeability.

Keywords: CO_2, Storage, Geochemistry, Reactive Transport

Introduction

Reactions between acidified, CO_2-rich brine stemming from subsurface CO_2 injection and formation mineralogy may lead to changes in porosity and permeability which could consequently impact injectivity. Because injection may utilize existing oil and gas wells constructed with standard oil well cement, the interaction of CO_2, brine, and the intrinsically alkaline cement composition must also be considered. Prior reactive transport modeling studies have addressed possible responses of reservoir mineralogy to CO_2 injection [1-4] while other studies entailing modeling and experimental approaches have focused on the potential reactions of injected CO_2 with wellbore cement [5-9]. The objective of this current research is to develop a geochemical model for the interaction of CO_2 with reservoir brine, formation minerals, and wellbore cement as constrained by site-specific field data and laboratory experiments for the Krechba gas field in central Algeria. The Krechba field is associated with the In Salah project, a joint venture between BP, and Statoil, and Sonatrach and currently one of the largest industrial-scale subsurface CO_2 storage projects in operation [10]. Since 2004, approximately one million tons per year of CO_2, recovered from extracted natural gas, has been injected at In Salah since 2004 through three wells screened within a 20-m thick fractured sandstone unit located at a depth of approximately 1,800 m.

As part of this study, we have conducted experiments that have entailed reacting sandstone and shale core samples collected from Krechba with brine, CO_2 and wellbore cement [11]. These experiments, which revealed solid phase compositional changes as well as changes in brine chemistry, have been used to posit specific mineral phases and associated reaction rates which react with CO_2. The resulting geochemical model was used to inform a reactive transport simulation of the near-wellbore

environment in response to CO_2 injection. Geochemical and reactive transport modeling were conducted with PHREEQC [12].

Reservoir Geochemistry: Mineralogy-Brine Equilibria and Interpretation of Experiments

The Krechba reservoir consists of a Carboniferous-age fractured fine-grained sandstone and siltsone. Armitage et al. [13] studied the mineralogical compositional variations among 17 core samples collected from the KB-502 boring at Krechba and reported compositions ranging from a quartz-dominated sandstone, with porosities on the order of 0.07 to 0.18, to shale-like material containing abundant illite clay, characterized by lower porosity values (0.02 to 0.04). An iron-rich chlorite, a likely product of diagenesis of Fe-rich 7Å clay deposited in an estuarine environment, is found in both the shale and sandstone (in the latter case as coatings on quartz grains) in abundances as high as 25 percent by volume. Other aluminosilicates include kaolinite (typically less than 5 percent by volume) and plagioclase-dominated feldspar, the latter reported only in trace amounts. Carbonate phases have been reported as siderite [13], ankerite and dolomite, or calcite (unpublished XRD analyses of Krechba core samples). Occasional barite has also been reported in some samples. The chemical composition of the Krechba brine is dominated by Na and Cl (up to approximately 3 molal), with significant concentrations of Ca and Mg also present (Table 1). Speciation of the brine chemistry with PHREEQC at the reservoir temperature of approximately 95°C using the extended Debye-Hückel activity coefficient correction model produced a set of saturation index values that are close to thermodynamic equilibrium for calcite, siderite, daphnite-7Å (an Fe-rich chlorite), albite, and gibbsite and slightly supersaturated with respect to illite, kaolinite, and dolomite.

Modeling the CO_2 reaction experiments involving shale and sandstone samples from KB-502 required assuming a set of primary mineral phases as well as inferred secondary reaction products. A kinetic dissolution rate expression of the form,

$$\frac{dM}{dt} = k\,A\left(\Omega - 1\right) \tag{1}$$

was utilized to model reaction kinetics, along with an equivalent expression for the kinetic precipitation rate,

$$\frac{dM}{dt} = k\,A\left(-\Omega^{-1}\right) \tag{2}$$

where M is the mineral mass, k the kinetic rate constant, A the mineral surface area, and,

$$\Omega = \frac{IAP}{K_{sp}} \tag{3}$$

Equation (3) defines the saturation ratio, Ω, of a particular phase, where *IAP* is the ion activity product of the constituent reactant and product species in the mineral phase's dissolution equation and K_{sp} the solubility product constant.

Concentrations of Fe, Si, and Al as a function of time for the shale and sandstone experiments are shown on Figure 1. We assumed that Fe concentration histories reflect the dissolution of an Fe-rich chlorite phase, represented in the model by daphnite-7Å, as published dissolution rates for siderite, which are typically on the order of 10^{-8} to 10^{-7} mol m^{-2} sec^{-1} [14], are too rapid to explain the long-term trends in the data. Increases in Al concentrations during the first 10 days, particularly evident in the shale data, are also consistent with the dissolution of an Al-bearing phase. Subsequent decreases in the Al in both experiments imply that other Al-bearing phase(s) must precipitate. We chose to model these possible secondary minerals as (1) a smectite phase, represented by calcium montmorillonite,

$Ca_{0.165}Mg_{0.33}Al_{1.67}Si_4O_{10}(OH)_2$, based upon the identification of an Fe-Mg-Al-Si-0 bearing secondary mineral phase (presumably a smectite) in some of the experiments, and (2) gibbsite, included to account for changes in Al concentrations in solution that could not be accommodated by the stoichiometry of other aluminosilicate phases. Platy crystals identified as precipitates in some experiments are morphologically consistent with gibbsite, but their composition could not be determined [11]. In addition, we assumed that a carbonate phase (calcite) existed in equilibrium with the brine over the course of the experiment, based on relatively rapid dissolution rates on the order of 10^{-6} to 10^{-7} mol m^{-2} sec^{-1} [15]. Based on observation [11], we also assumed that an amorphous SiO_2 phase appeared in the sandstone experiment and included it in the model as an equilibrium phase based on a reported dissolution rate on the order of 10^{-9} mol m^{-2} sec^{-1} [16]. Finally, both the sandstone and shale models assumed that dissolved CO_2 concentrations reflected equilibrium with a CO_2 gas phase fugacity corresponding to 200 bars, calculated via the model of Duan and Sun [17].

Lumped values for $k \cdot A$ (Eqs. 1 and 2) which best match the concentration histories of Fe, Si, and Al (Figure 1) include 9 x 10^{-11} mol/sec and 6.5 x 10^{-11} mol/sec for the daphnite in the shale and sandstone experiments, respectively, 5.8 x 10^{-11} mol/sec for calcium montmorillonite (both experiments), and 3.7 x 10^{-11} mol/sec for gibbsite (both experiments). Assuming a spherical particle in the middle of the silt size range (e.g., d = 20 µm), a particle density of 2.6 g/cm^3, a rock:water mass ratio of 0.1 g/g (as imposed by the experiments), and a mean chlorite volume fraction abundance of 0.2 yields a surface area of approximately 0.9 m^2/L of water. This would suggest that the chlorite dissolution rates in our experiments, normalized by surface area, are on the order of 1 x 10^{-11} to 2 x 10^{-11} mol m^{-2} sec^{-1}. For comparison, Brandt et al. [18] reported dissolution rates for Mg-rich chlorite on the order of 4- to 7 x 10^{-11} mol m^{-2} sec^{-1}, calculated for reactive mineral surface area at pH 2 and 25°C for an Mg-rich chlorite.

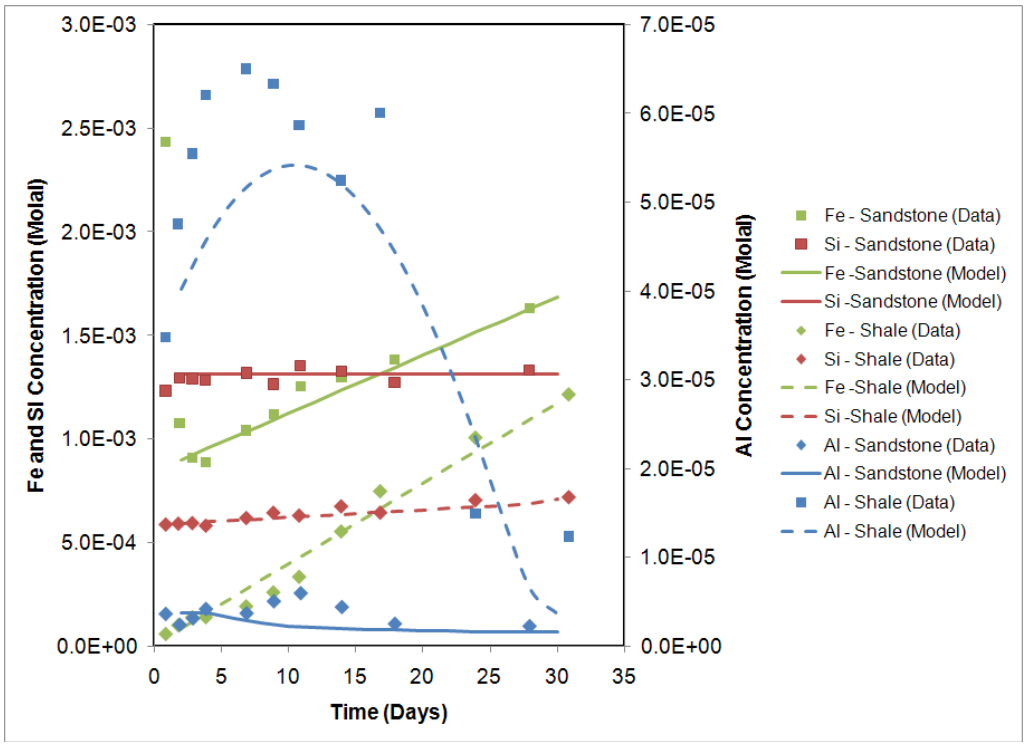

Figure 1. Measured and modeled concentrations of Fe, Si, and Al in sandstone and shale experiments as a function of time.

Wellbore Cement

A separate geochemical model for the wellbore cement was developed for the hydration and carbonation phases of the brine-cement-CO_2 experiments described by Carroll et al. [11]. As an initial condition, we assumed that the Ca-Si-Al oxide components of a typical Class G oil well cement (Lehigh Inland Cement, Edmonton, Alberta, Canada), comprised of 46% Ca_3SiO_5 ("C3S"), 37% Ca_2SiO_4 ("C2S"), 7.2% SO_3, 4.7% MgO, 3.4% $(CaO)_3(Al_2O_3)$, 1.7% Na_2O, and 0.5% $(CaO)_3(Fe_2O_3)$, were added as reactants to the synthetic brine composition in accordance with the cement:brine mixing ratio used in the experiments (e.g., 1:10, by mass). Candidate mineral phases were then evaluated by simulating equilibration with the brine and comparing the results to the changes in brine chemistry observed during the hydration phase, assuming complete hydration. Subsequently, the hydrated mineral assemblage and the associated brine were equilibrated with CO_2 gas at a fugacity corresponding to 200 bars, with a set of carbonated cement minerals replacing the hydrated cement phases.

A postulated hydrated cement mineral assemblage consisting of portlandite, jennite (including an Mg-jennite component) – $Ca_{1.67}SiO_2(OH)_{3.33}$:$0.43H_2O$, as a calcium-silicate-hydrate ("C-S-H") proxy, monosulfoaluminate – $Ca_4Al_2O_6(SO_4)$:$12H_2O$, an Fe-hydrogarnet – $Ca_3Fe_2(OH)_{12}$, and ettringite – $Ca_6Al_2(SO_4)_3(OH)_{12}$:$26H_2O$, was used to model the hydrated cement, based upon (1) similar mineralogical models utilized in prior studies [9,19], and (2) agreement between simulated and observed final concentrations of Al, Fe, Si, and Ca characterizing the hydration experiment (Figure 2). For the carbonation phase of the experiment, we assumed that both calcite and amorphous SiO_2 comprised the majority of the carbonation products based on the observed prevalence of these phases among the cement carbonation products. Other assumed reaction products included $Fe(OH)_3$, amorphous $Al(OH)_3$, and gypsum.

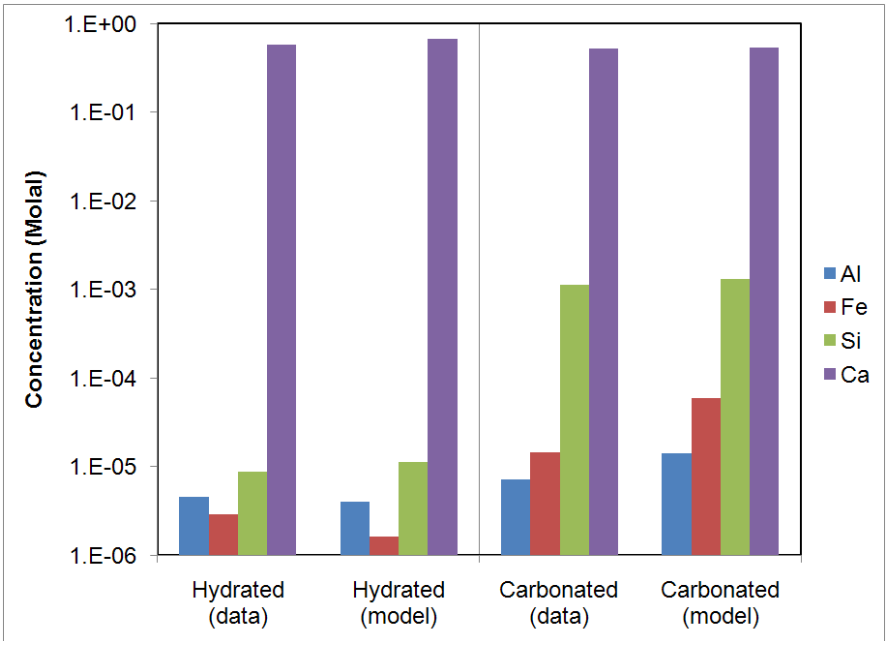

Figure 2. Measured and modeled concentrations of Fe, Si, Al, and Ca in simulated experimental brine in equilibrium with posited hydrated and carbonated cement mineral phases.

Reactive Transport Model for the Cement-Formation Interface

To assess changes in mineralogy and porosity at the wellbore cement interface, we employed a dual porosity modeling approach which assumed advective solute transport through the formation material and Fickian diffusion into and out of the cement. Key assumptions included:

- A 50-m-long column of reservoir formation material was discretized into 50 1-m cells.
- Each cell was associated with an "immobile porosity" cell, representing an adjacent portion of wellbore cement. Diffusive solute transport between the formation material and cement was quantified using a mass transfer coefficient [20] and included an assumed 1-cm thickness for the reactive zone, a cement porosity of 0.30 and a tortuosity equivalent to 0.004 [5], an aqueous diffusion coefficient of 10^{-9} m^2/sec for all dissolved components, and a shape factor for flow past a thin cylinder.
- The brine mixture entering the column consisted of (1) Krechba brine equilibrated with CO_2 in the presence of calcite, and (2) a fictitious supercritical CO_2 species mixed with the brine at a concentration of 2.8 mol/L, corresponding to a 25% supercritical CO_2 fluid fraction, by weight, based on a density of 0.5 gm/L and a molecular weight of 0.044 kg/mol.
- One pore volume was flushed through the column by advection every 100 days, equivalent to a formation permeability of 7.4 millidarcies (consistent with unpublished Krechba matrix permeability estimates obtained from core experiments) and a pressure drop of approximately 10 bars across the column.
- Formation material was assumed to be a compositional average of the shale and sandstone end members.
- The initial cement composition is based on the simulated hydration of Class G anhydrous oxide components in comparatively dilute shallow groundwater.

The position of the CO_2 front in the formation material adjacent to the cement after 8 years is shown on Figure 3; the impact on the cement mineralogy is shown on Figure 4. Carbonation of the cement is indicated by the replacement of portlandite and jennite by calcite and amorphous SiO_2, along with a number of other mineralogical changes among minor cement constituents. The result is a minor porosity increase in the cement at the column inlet and a porosity decrease further downgradient (Figure 5). The net impact of reactions and diffusive mass transfer on the formation mineral assemblage is shown on Figure 6 and includes (1) a loss of calcite from the upgradient end of the column, (2) precipitation of siderite, calcite, and magnesite further downgradient within the column, and (3) precipitation of gibbsite, calcium montmorillonite, and amorphous SiO_2 in various proportions, depending on reaction kinetics assumptions. The net impact of the volume changes associated with all mineral precipitation and dissolution reactions is shown on Figure 5. The implied net porosity increase in the formation materials is comparatively minor over this time scale, amounting to less than 1 percent of the total solid volume. Taken together, projected porosity changes in the cement (with an intrinsically negligible permeability), and in the downgradient portion of the adjacent formation material imply that an overall increase in permeability of the interface region is not expected, indicating that the cement-formation interface will not likely present a preferential escape path for CO_2.

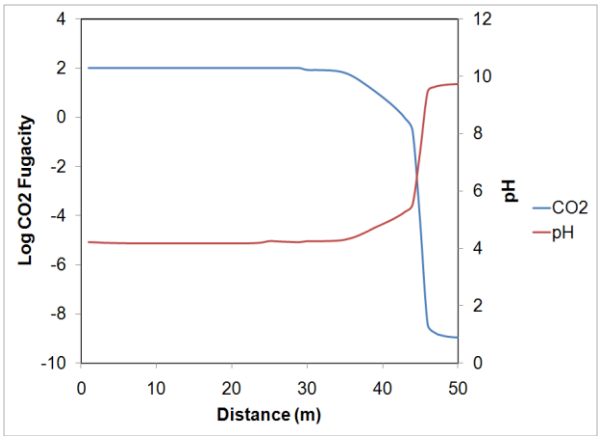

Figure 3. Position of the CO_2 front, and zone of accompanying low pH, within the formation material after 8 years or approximately 30 pore volumes of flushed brine + CO_2.

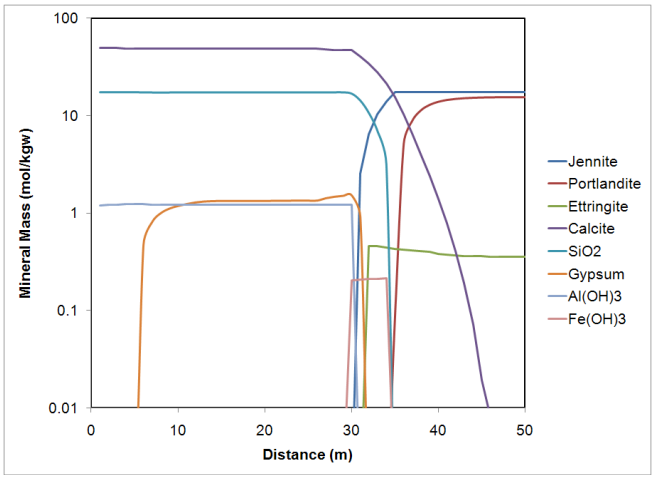

Figure 4. Simulated mineralogical changes in cement adjacent to formation material after 8 years or approximately 30 pore volumes of flushed brine + CO_2.

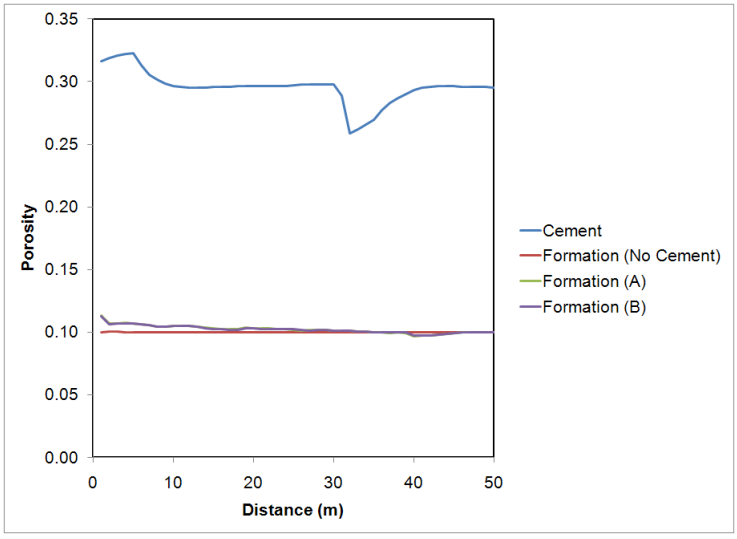

Figure 5. Simulated changes in porosity in cement and formation materials, based on estimated mineral molar volumes, after 8 years or approximately 30 pore volumes of flushed brine + CO_2. Case "A" assumes reaction kinetics determined from batch experiments on sandstone/shale samples; Case "B" assumes rapid Ca-montmorillonite precipitation (equilibrium) in presence of cement. "Formation (No Cement)" is a reference simulation for dual-porosity transport through formation material in the absence of cement.

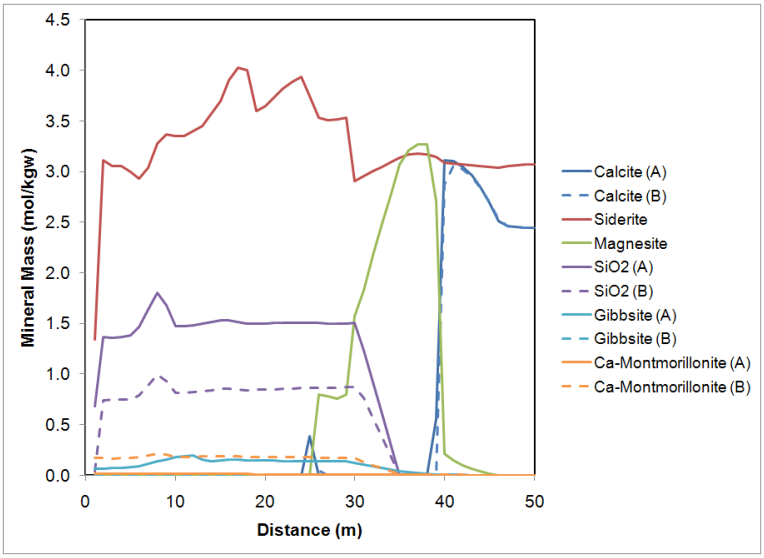

Figure 6. Simulated mineralogical changes in the formation material after 8 years or approximately 30 pore volumes of flushed brine + CO_2. Calcite and siderite are initially present at 2.4 and 3.1, mole/kg of water, respectively. Case "A" assumes reaction kinetics determined from batch experiments on sandstone/shale samples; Case "B" assumes rapid Ca-montmorillonite precipitation (equilibrium) in presence of cement.

Acknowledgements

This work was performed under the auspices of the U.S. Department of Energy by Lawrence Livermore National Laboratory under Contract DE-AC52-07NA27344. We acknowledge funding from the Joint Industry Project (a consortium consisting of BP, Statoil and Sonatrach) and the U.S. Department of Energy to investigate the importance of geochemical alteration at the In Salah CO_2 storage project.

List of References

- [1] Gunter WD, Wiwchar B, Perkins EH. Aquifer disposal of CO_2-rich greenhouse gases: extension of the time scale of experiment for CO_2-sequestering reactions by geochemical modeling. Mineralogy and Petrology 1997; 59: 121–140.
- [2] Johnson JW, Nitao JJ, Steefel CI, Knaus KG. Reactive transport modeling of geologic CO_2 sequestration in saline aquifers: the influence of intra-aquifer shales and the relative effectiveness of structural, solubility, and mineral trapping during prograde and retrograde sequestration, In Proceedings of the 1st National Conference on Carbon Sequestration, 2001. Washington, DC.
- [3] White SP, Weir GJ, Kissling WM. Numerical simulation of CO_2 sequestration in natural CO_2 reservoirs on the Colorado Plateau, in Proceedings of the 1st National Conference on Carbon Sequestration, 2001. Washington, DC.
- [4] Xu, T, Kharaka YK, Doughty C, Freifeld BM, Daley TM. Reactive transport modeling to study changes in water chemistry induced by CO_2 injection at the Frio-I Brine Pilot. Chemical Geology 2010; 271: 153–164.
- [5] Carey JW, Wigand M, Chipera SJ, WoldeGabriel G, Pawar R, Lichtner PC, Wehner SC, Raines MA, Guthrie GD. Analysis and performance of oil well cement with 30 years of CO_2 exposure from the SACROC Unit, West Texas, USA. International Journal of Greenhouse Gas Control 2007; 1: 75–85.
- [6] Kuthcko, BG, Strazisar BR, Dzombak DA, Lowry GV, N. Thaulow. Degradation of well cement by CO_2 under geologic sequestration conditions. Environmental Science and Technology 2007; 41: 4787-4792.

- [7] Duguid A. An estimate of the time to degrade the cement sheath in a well exposed to carbonated brine. Energy Procedia 2009; 3181–3188.
- [8] Wigand, M, Kaszubab JP, Carey JW, Hollis WK. Geochemical effects of CO_2 sequestration on fractured wellbore cement at the cement/caprock interface. Chemical Geology 2009; 265: 122-133.
- [9] Huet BM, Prevost JH, Scherer GW. Quantitative reactive transport modeling of Portland cement in CO_2-saturated water, International Journal of Greenhouse Gas Control 2010; doi:10.1016/j.ijggc.2009.11.003.
- [10] Ringrose P, Atbi M, Mason D, Espinassous M, Myhrer Ø, Iding M, Mathieson A, Wright I. Plume development around well KB-502 at the In Salah CO_2 storage site. First Break 2009; 27: 85–89.
- [11] Carroll S, W McNab. Wellbore Integrity in at Krechba: 1. Experimental Study of Cement – Sandstone/Shale– Brine – CO_2. Int. Conference on Greenhouse Gas Technologies, 2010 (GHGT-10); www.sciencedirect.com.
- [12] Parkhurst DL, Appelo CAJ. *User's Guide to PHREEQC (Version 2)--A Computer Program for Speciation, Batch-reaction, One-dimensional Transport, and Inverse Geochemical Calculations*. U.S. Geological Survey Water-Resources Investigations Report 99-4259, 1999. 312 p.
- [13] Armitage PJ, Worden RH, Faulkner DR, Aplin AC, Butcher AR, and Iliffe J. Diagenetic and sedimentary controls on porosity in Lower Carboniferous fine-grained lithologies, Krechba field, Algeria: A petrological study of a caprock to a carbon capture site. Marine and Petroleum Geology 2010; in press: doi:10.1016/j.marpetgeo.2010.03.01.
- [14] Golubev SV, Bénézeth P, Schott J, Dandurand JL, Castillo A. Siderite dissolution kinetics in acidic aqueous solutions from 25 to 100 °C and 0 to 50 atm pCO_2. Chemical Geology 2009; 265: 13–19.
- [15] Svensson U, Dreybrodt W. Dissolution kinetics of natural calcite minerals in CO_2-water systems approaching calcite equilibrium. Chemical Geology 1992; 100: 129–145.
- [16] Carroll S, Mroczek E, Alai M, Ebert M. Amorphous silica precipitation (60 to 120°C): Comparison of laboratory and field rates. Geochimica et Cosmochimica Acta 1998; 62: 1379–1396.
- [17] Duan Z, Sun R. An improved model calculating CO_2 solubility in pure water and aqueous NaCl solutions from 273 to 533 K and from 0 to 2000 bar. Chemical Geology 2003; 193: 257-271.
- [18] Brandt F, Bosbach D, Krawczyk-Bärsch E, Arnold T, Bernhard G. Chlorite dissolution in the acid ph-range: a combined microscopic and macroscopic approach. Geochimica et Cosmochimica Acta 2003; 67: 1451-146.
- [19] García VE. *Estabilitat de la Dolomita en el Medi de la Pasta Pòrtland: Aplicació a la Fabricació de Formigons amb Àrids Dolomítics*. Ph.D. Dissertation, 2004. University of Barcelona.
- [20] Van Genuchten M. A general approach for modeling solute transport in structured soils, Memoires of the International Association of Hydrogeologists 1985; 17: 513-526.